27th EUSIPCO 2019
European Signal Processing Conference
A Coruña, Spain, September 2-6, 2019

Second-order time-reassigned synchrosqueezing: Application to Draupner wave analysis

Dominique Fourer and François Auger

September 5, 2019

ibisc
université evry val-d'essonne
université PARIS-SACLAY
IREENA Institut de Recherche en Energie Electrique de Nantes Atlantique - EA 4642
UNIVERSITÉ DE NANTES

Purpose of this work

Goals

- Computing efficient representations for handling non-stationary multicomponent signals
- Dealing with impulsive-like and/or strongly modulated signals
- Reversible representation allowing an extraction of the elementary signal components
- Meaningful **information extraction** from observation

$\Rightarrow$ **Proposed approach:** Time-frequency analysis combined with reassignment-based post-processing methods (i.e. synchrosqueezing)

Context of our research: the ASTRES project 2014-2017 funded by the French ANR

ASTRES: Analysis, Synthesis and Transformation by Reassignment, EMD and Synchrosqueezing.

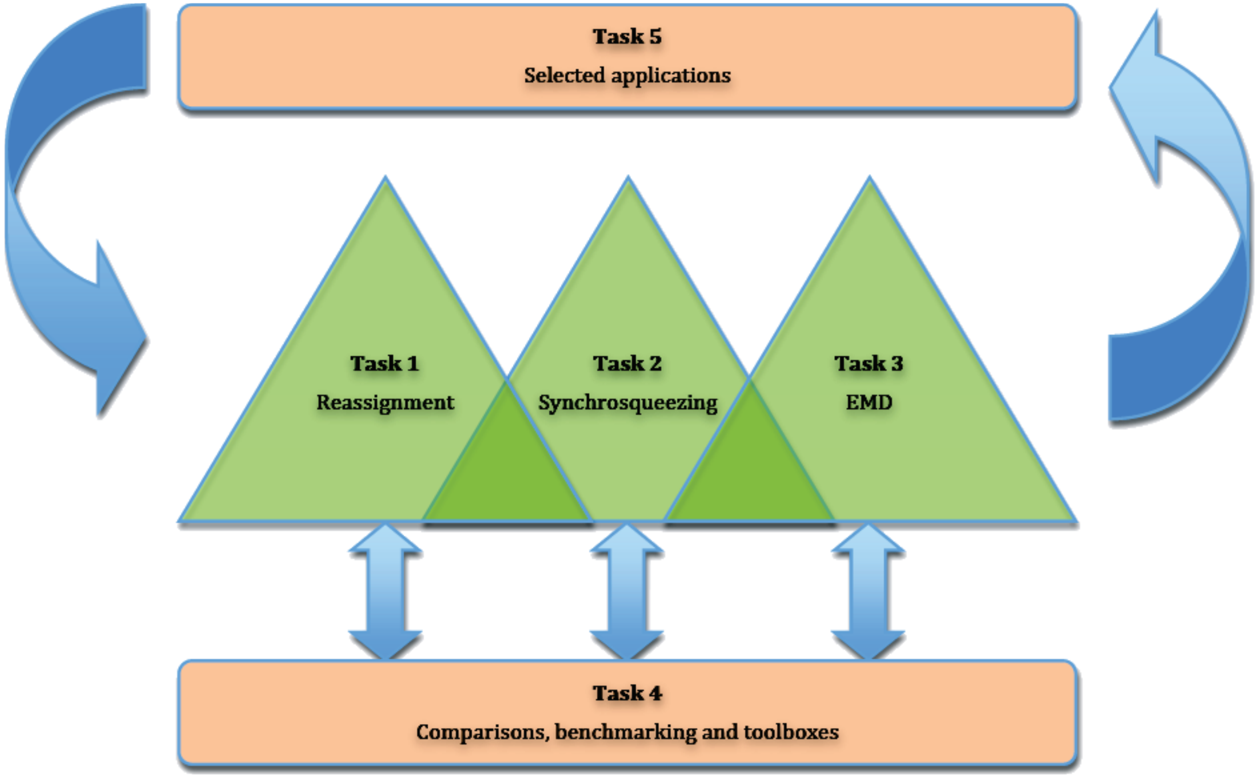

Offers a new toolbox for non-stationary multicomponent signal processing:
`https://github.com/dfourer/ASTRES_toolbox`

D. Fourer, J. Harmouche, J. Schmitt, T. Oberlin, S. Meignen, F. Auger and P. Flandrin. The ASTRES Toolbox for Mode Extraction of Non-Stationary Multicomponent Signals. Proc. EUSIPCO 2017, Aug. 2017. Kos Island, Greece.

The new French ANR ASCETE project: 2019-2022

ASCETE: Analysis and Separation of Complex signal: Exploiting the Time-frequency structurE

Project holder: Sylvain Meignen (LJK, Grenoble)

- Extends the previous methods with stochastic models
- Combines signal processing methods with machine learning
- New applications to audio, biomedicine, astrophysics, etc.

Plan

1. Introduction
2. Time-reassigned synchrosqueezing
   - Rationale
   - Second-order time-reassigned synchrosqueezing
3. Application to Draupner wave analysis
   - Data description
   - Application to Draupner wave analysis
4. Conclusion

STFT definitions

- We define the STFT of a signal x as a function of time t and frequency ω computed using a differentiable analysis window h as:

$$F_x^h(t,\omega) = \int_{\mathbb{R}} x(\tau)h(t-\tau)^* \, \mathbf{e}^{-j\omega\tau} \, \mathrm{d}\tau \tag{1}$$

  with $j^2{=}{-1}$ the imaginary unit and z^* the complex conjugate of z.
- A time-frequency representation is provided by the spectrogram defined as: $|F_x^h(t,\omega)|^2$.
- Signal reconstruction formula:

$$x(t) = \frac{1}{2\pi h(0)^*} \int_{\mathbb{R}} F_x^h(t,\omega) \, \mathbf{e}^{j\omega t} d\omega \tag{2}$$

  when $h(0) \neq 0$

The reassignment method [Kodera *et al.* 1978] [Auger,Flandrin, 1995]

Principle

Improves the readability of a time-frequency representation (TFR):
Reassignment moves the signal energy according to: $(t,\omega) \mapsto (\hat{t}_{x(t,\omega)}, \hat{\omega}_{x(t,\omega)})$, where $\hat{t}_x(t,\omega)$ is a group-delay estimator and $\hat{\omega}_x(t,\omega)$ is an instantaneous frequency estimator.

Both time-frequency reassignment operators can be computed as follows (STFT case):

$$\hat{t}_{x(t,\omega)} = \mathrm{Re}\left(\tilde{t}_{x(t,\omega)}\right), \text{with} \quad \tilde{t}_{x(t,\omega)} = t - \frac{F_x^{\mathcal{T}h}(t,\omega)}{F_x^h(t,\omega)} \tag{3}$$

$$\hat{\omega}_{x(t,\omega)} = \mathrm{Im}\left(\tilde{\omega}_{x(t,\omega)}\right), \text{with} \quad \tilde{\omega}_{x(t,\omega)} = j\omega + \frac{F_x^{\mathcal{D}h}(t,\omega)}{F_x^h(t,\omega)} \tag{4}$$

where $\mathcal{T}h(t) = th(t)$ and $\mathcal{D}h(t) = \frac{dh}{dt}(t)$ are modified versions of the analysis window h.
The reassigned spectrogram is computed by:

$$\mathrm{RF}_x^h(t,\omega) = \iint_{\mathbb{R}^2} |F_x^h(\tau,\Omega)|^2 \delta\left(t - \hat{t}_x(\tau,\Omega)\right) \delta\left(\omega - \hat{\omega}_x(\tau,\Omega)\right) \mathrm{d}\tau \mathrm{d}\Omega. \tag{5}$$

The resulting reassigned spectrogram $\mathrm{RF}_x(t,\omega)$ is a sharpened but non-reversible TFR due to the loss of the phase information.

The reassigned spectrogram

$$R_x(t,\omega) = \iint_{\mathbb{R}^2} \left| F_x^h(\tau,\Omega) \right|^2 \delta(t - \hat{t}(\tau,\Omega))\delta(\omega - \hat{\omega}(\tau,\Omega))\, d\tau \frac{d\Omega}{2\pi} \tag{6}$$

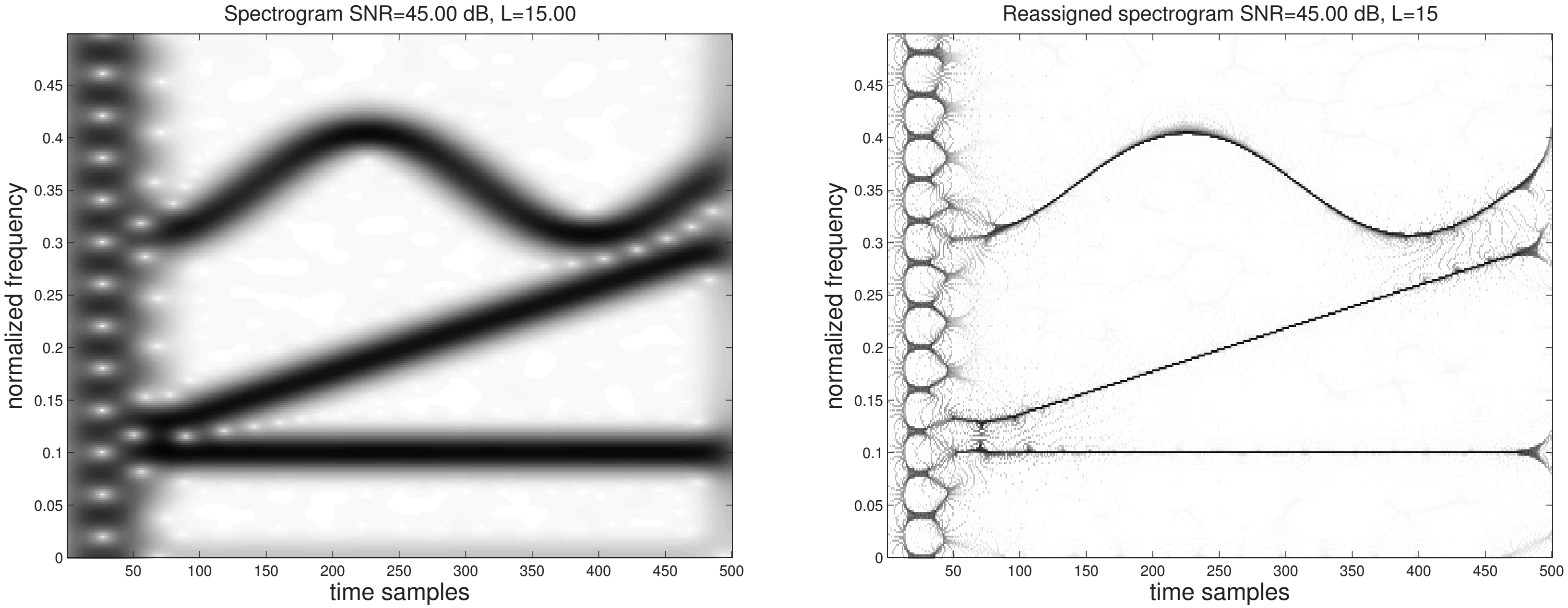

(a) $|F_x^h(t,\omega)|^2$

(b) $R_x^h(t,\omega)$

Synchrosqueezing [Daubechies 1996, 2011] [Thakur 2011]

Principle

A variant of the reassignment method to compute sharpen and reversible TFRs by reassigned the transform instead of its energy to preserve the phase information.

Computation of the synchrosqueezed STFT:

$$S_x(t,\omega) = \frac{1}{h(0)} \int_{\mathbb{R}} F_x^h(t,\Omega)\delta(\omega - \hat{\omega}(t,\Omega))\, \frac{d\Omega}{2\pi} \tag{7}$$

Its signal reconstruction formula:

$$\hat{x}(t) = \int_{\mathrm{supp}_\Omega(x)} S_x(t,\Omega) d\Omega \tag{8}$$

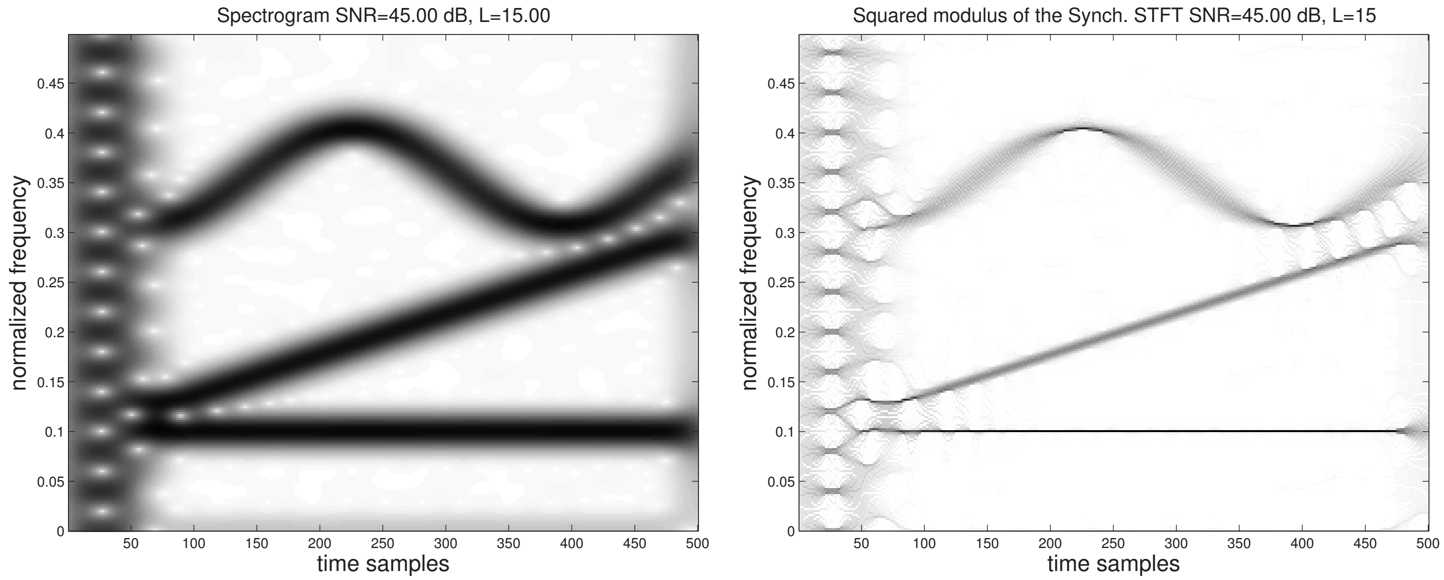

Mode extraction

Principle

Apply a time-frequency mask over a previously computed reversible TFR.
$\Rightarrow$ Performs better if the components are sparse and well disentangled.

[Brevdo, 2011] method finds the best frequency curve $\Omega(t)$ to maximizes the energy with a smooth constraint through a total variation penalization term:

$$\hat{\Omega} = \underset{\Omega}{\operatorname{argmax}} \int_{\mathbb{R}} |S_x(t, \Omega(t))|^2 \, dt - \lambda \int_{\mathbb{R}} \left| \frac{d\Omega}{dt}(t) \right|^2 dt, \quad (9)$$

where λ controls the importance of the smoothness of Ω.

Notice: When the ridges of several components have to be estimated, this method can be iterated after subtracting the energy located at the previously estimated ridge.

STFT properties

The STFT marginalization over time of $F_x^h(t,\omega)$ leads to:

$$\int_{\mathbb{R}} F_x^h(t,\omega)\,dt = \iint_{\mathbb{R}^2} h(t-\tau)^* x(\tau)\,\mathbf{e}^{-j\omega\tau}\,dtd\tau \tag{10}$$

$$= \iint_{\mathbb{R}^2} h(u)^* x(\tau)\,\mathbf{e}^{-j\omega\tau}\,dud\tau \tag{11}$$

$$= \int_{\mathbb{R}} h(u)^*\,du \int_{\mathbb{R}} x(\tau)\,\mathbf{e}^{-j\omega\tau}\,d\tau \tag{12}$$

$$= F_h(0)^* F_x(\omega) \tag{13}$$

with $F_x(\omega) = \int_{\mathbb{R}} x(t)\,\mathbf{e}^{-j\omega t}\,dt$ the Fourier transform of signal x.
Hence, the signal can be recovered by:

$$x(t) = \frac{1}{2\pi F_h(0)^*} \iint_{\mathbb{R}^2} F_x(\tau,\omega)\,\mathbf{e}^{j\omega t}\,d\tau d\omega \tag{14}$$

Time-reassigned synchrosqueezed STFT [He 2019]

Principle

Synchrosqueezes the original transform along the time axis instead of the frequency axis exploiting the STFT properties when marginalized over time.

The time-reassigned synchrosqueezed STFT can be defined as:

$$T_x^h(t,\omega) = \int_{\mathbb{R}} F_x^h(\tau,\omega)\delta\left(t - \hat{t}_x(\tau,\omega)\right)\, d\tau \tag{15}$$

where $\hat{t}_x(t,\omega)$ corresponds to a group-delay estimator related to the time reassignment operator given by Eq. (3).
The original signal can thus be reconstructed using the following exact formula:

$$x(t) = \frac{1}{2\pi F_h(0)^*} \iint_{\mathbb{R}^2} T_x^h(\tau,\omega)\, \mathbf{e}^{j\omega t}\, d\tau d\omega \tag{16}$$

Numerical results

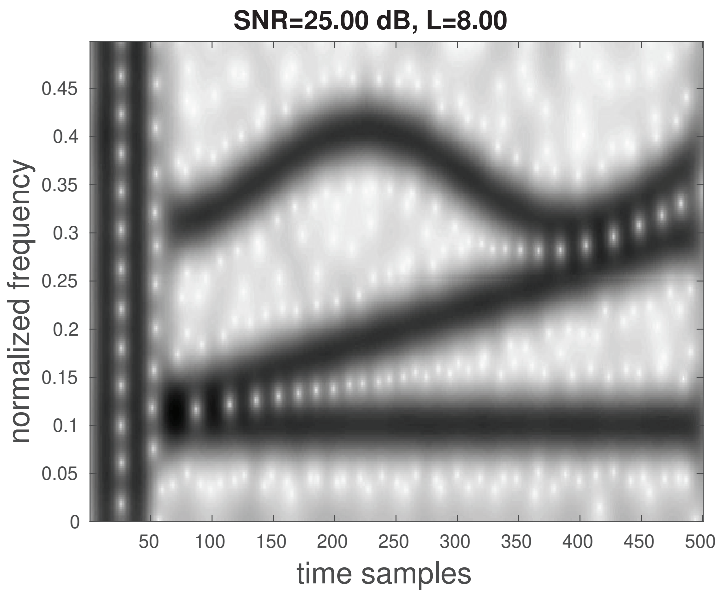

(e) $|F_x^h(t,\omega)|^2$

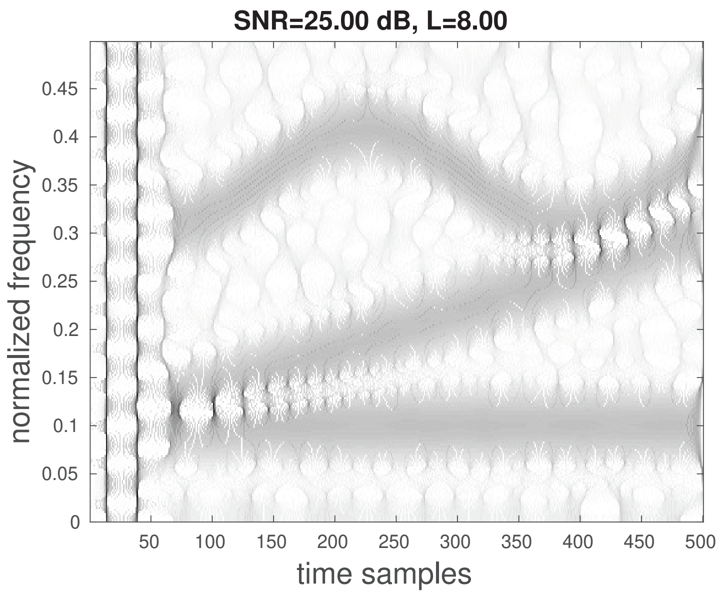

(f) $|T_x^h(t,\omega)|^2$

- Perfect localization of the 2 impulses
- Poor localization of the sinusoidal components

Signal model

$$x(t) = \mathbf{e}^{\lambda_x(t)+j\phi_x(t)} \quad (17)$$

$$\text{with} \quad \lambda_x(t) = l_x + \mu_x t + \nu_x \frac{t^2}{2} \quad (18)$$

$$\text{and} \quad \phi_x(t) = \varphi_x + \omega_x t + \alpha_x \frac{t^2}{2} \quad (19)$$

where $\lambda_x(t)$ and $\phi_x(t)$ respectively stand for the log-amplitude and phase and with $q_x = \nu_x + j\alpha_x$ and $p_x = \mu_x + j\omega_x$.

For such a signal, it can be shown that [Fourer et al., 2017]:

$$\omega_x = \text{Im}(\tilde{\omega}_{x(t,\omega)} - q_x \, \tilde{t}_{x(t,\omega)}) = \hat{\omega}_{x(t,\omega)} - \text{Im}(q_x \, \tilde{t}_{x(t,\omega)}) \quad (20)$$

Enhanced group-delay estimation

The new proposed second-order horizontal synchrosqueezing consists in moving $F_x^h(t,\omega)$ from the point (t,ω) to the point $(t_x^{(2)},\omega)$ located on the instantaneous frequency curve, *i.e.* such that $\dot{\phi}(t_x^{(2)}) = \frac{d\phi_x}{dt}(t_x^{(2)}) = \omega_x + \alpha_x t_x^{(2)} = \omega$.

This leads to:

$$t_x^{(2)} = \frac{\omega - \omega_x}{\alpha_x} = \hat{t}_x(t,\omega) + \frac{\omega - \hat{\omega}_x(t,\omega)}{\alpha_x} + \frac{\nu_x}{\alpha_x}\mathrm{Im}(\tilde{t}_x(t,\omega)) \tag{21}$$

which can be estimated by:

$$\hat{t}_x^{(2)}(t,\omega) = \begin{cases} \frac{\omega - \hat{\omega}_x(t,\omega) + \mathrm{Im}(\hat{q}_x(t,\omega)\,\tilde{t}_x(t,\omega))}{\hat{\alpha}_x(t,\omega)} & \text{if } \hat{\alpha}_x(t,\omega) \neq 0 \\ \hat{t}_x(t,\omega) & \text{otherwise} \end{cases} \tag{22}$$

where $\hat{q}_x(t,\omega) = \hat{\nu}_x(t,\omega) + j\hat{\alpha}_x(t,\omega)$ is an unbiased estimator of q_x.

Implementation considerations

In [Fourer et al.,2017] and [Fourer et al., 2018] we introduced two families of unbiased estimators called (tn) and (ωn) involving n-order derivatives $(n \geq 2)$ with respect to time (resp. to frequency) which enable to compute Eqs. (22).

$$\hat{q}_x^{(tn)}(t,\omega) = \frac{F_x^{\mathcal{D}^n h} F_x^h - F_x^{\mathcal{D}^{n-1} h} F_x^{\mathcal{D}h}}{F_x^{\mathcal{T}h} F_x^{\mathcal{D}^{n-1}h} - F_x^{\mathcal{T}\mathcal{D}^{n-1}h} F_x^h} \quad (23)$$

$$\hat{q}_x^{(\omega n)}(t,\omega) = \frac{(F_x^{\mathcal{T}^{n-1}\mathcal{D}h} + (n-1) F_x^{\mathcal{T}^{n-2}h}) F_x^h - F_x^{\mathcal{T}^{n-1}h} F_x^{\mathcal{D}h}}{F_x^{\mathcal{T}^{n-1}h} F_x^{\mathcal{T}h} - F_x^{\mathcal{T}^n h} F_x^h} \quad (24)$$

with $\mathcal{D}^n h(t) = \frac{d^n h}{dt^n}(t)$ and $\mathcal{T}^n h(t) = t^n h(t)$.

- discrete-time reformulations of our previously described expressions combined with the rectangle approximation method. Thus $F_x^h[k,m] \approx F_x^h(\frac{k}{F_s}, 2\pi \frac{mF_s}{M})$, where F_s denotes the sampling frequency, $k \in \mathbb{Z}$ is the time sample index and $m \in \mathcal{M}$ is the discrete frequency bin.
- The number of frequency bins M is chosen as an even number such as $\mathcal{M} = [-M/2+1; M/2]$
- Our implementation uses a Gaussian window expressed as $h(t) = \frac{1}{\sqrt{2\pi}T} \mathbf{e}^{-\frac{t^2}{2T^2}}$ where T is the time-spread of the window which can be related to $L = TF_s$.

Comparative numerical results 1/2

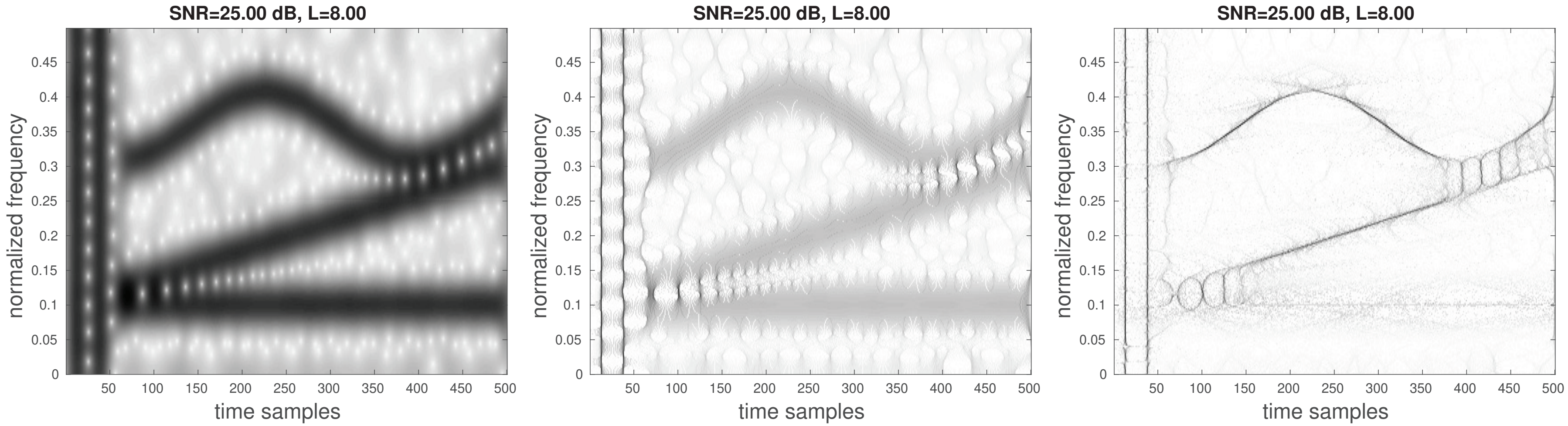

(g) spectrogram

(h) time-reassigned synchrosqueezing

(i) second-order horizontal synchrosqueezing

Comparative numerical results 2/2

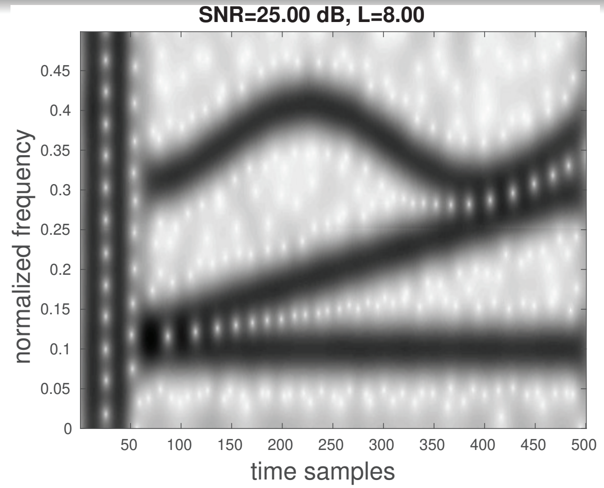

(j) spectrogram

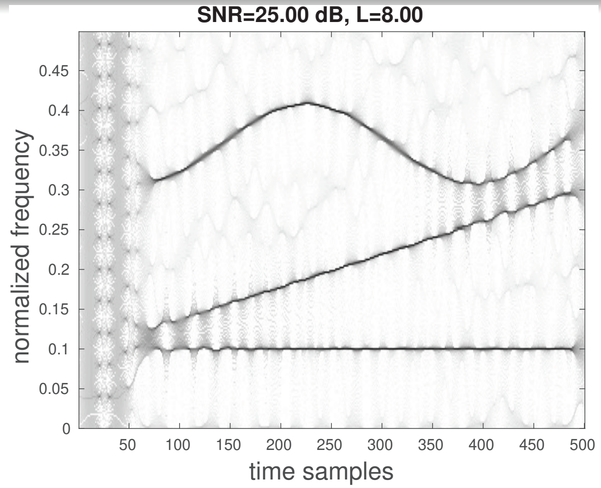

(k) synchrosqueezing

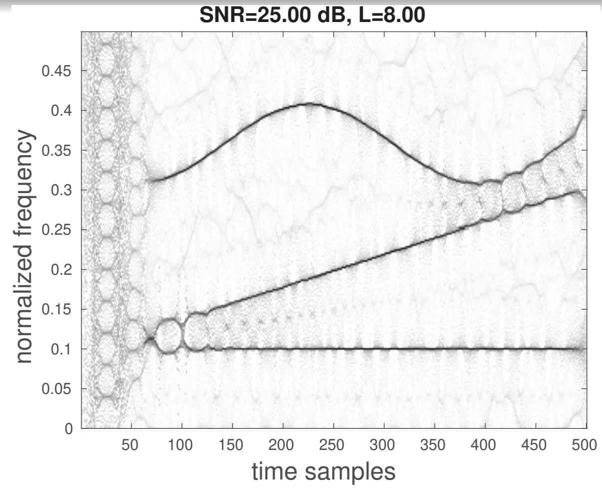

(l) second-order vertical synchrosqueezing

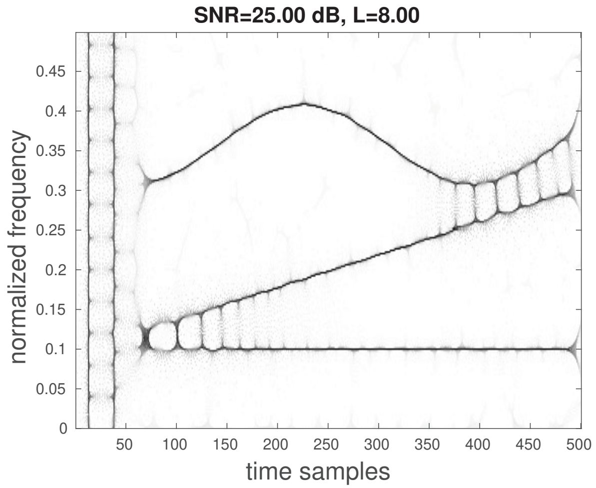

(m) reassignment

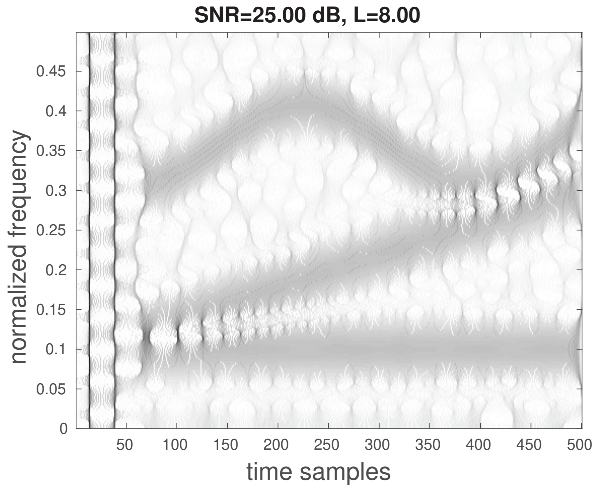

(n) time-reassigned synchrosqueezing

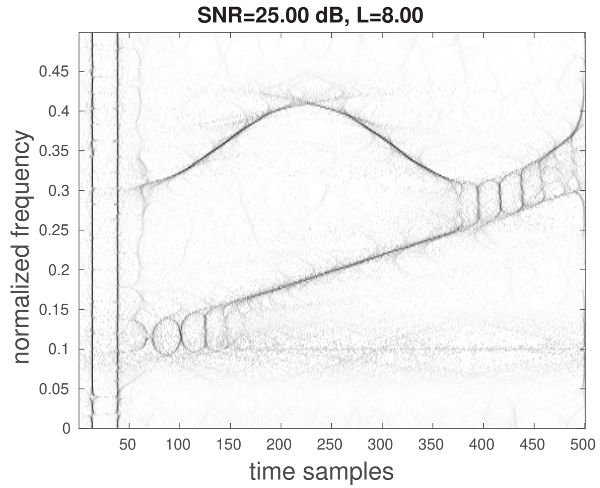

(o) second-order horizontal synchrosqueezing

Signal reconstruction

Whole signal reconstruction expressed in terms of Reconstruction quality Factor (RQF):

$$\mathrm{RQF} = 10\log_{10}\left(\frac{\sum_n |x[n]|^2}{\sum_n |x[n]-\hat{x}[n]|^2}\right) \quad (25)$$

Method	RQF (dB)
STFT	269.27
reassignment	N/A
classical synchrosqueezing	35.89
second-order vertical synchrosqueezing	23.80
time-reassigned synchrosqueezing	116.67
second-order time-reassigned synchrosqueezing	116.67

Draupner wave recording

We consider a possible freak wave event measured in the North Sea on the Draupner Platform the 1st of january 1995.

Draupner wave signal [Haver, 2004]

- The signal corresponds to the sea surface elevation deduced from the measures provided by a wave sensors consisting of a down-looking laser.
- The sampling frequency of this signal is $F_s = 2.13$ Hz and the duration is 20 minutes.

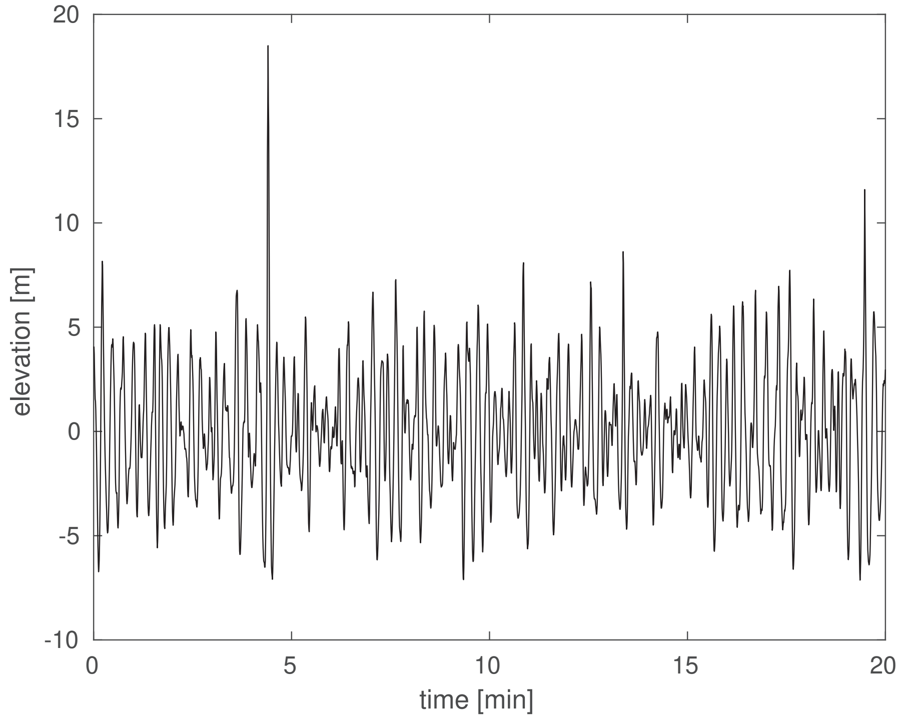

(p) $x(t)$

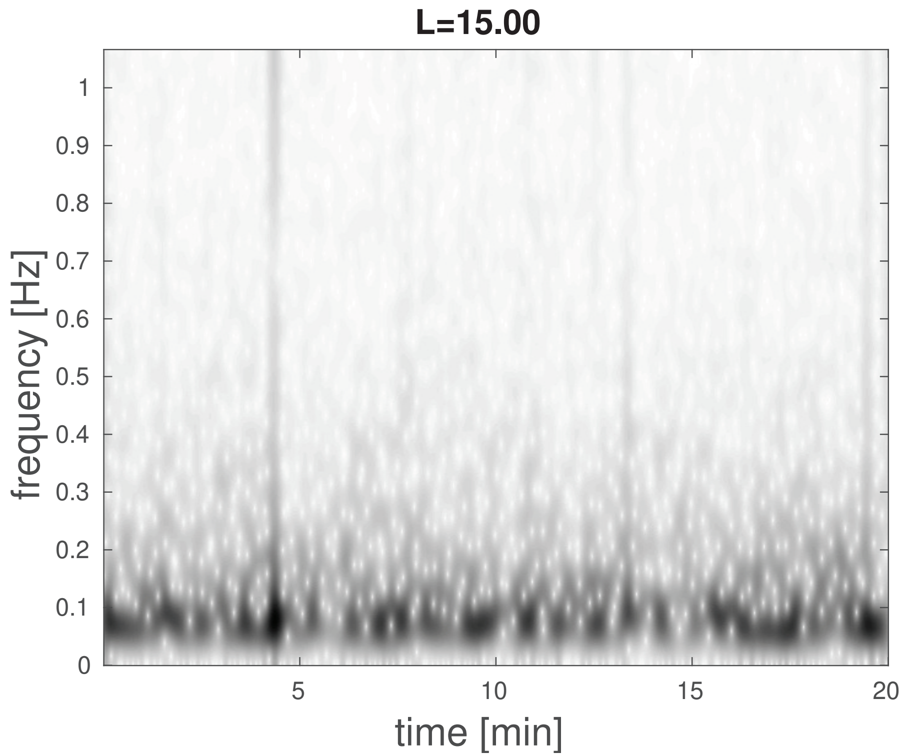

(q) $|F_x(t, \omega)|^2$

Time-frequency representations

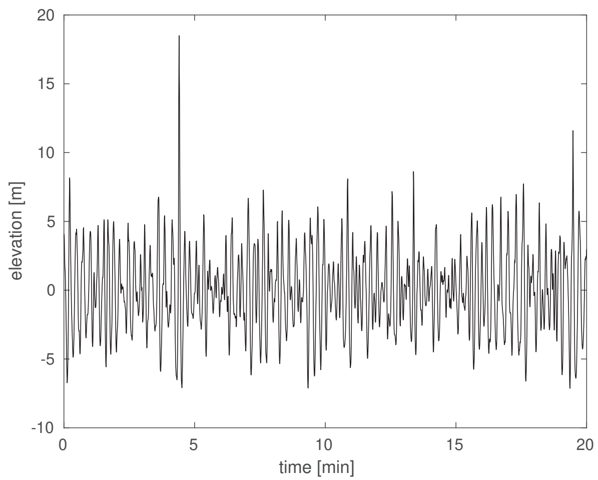

(r) signal

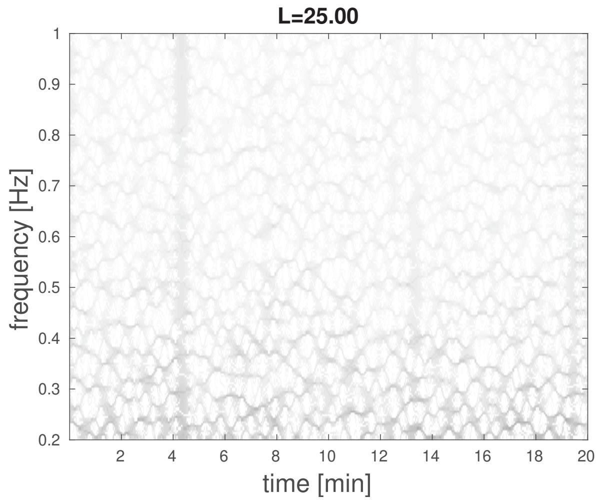

(s) synchrosqueezing

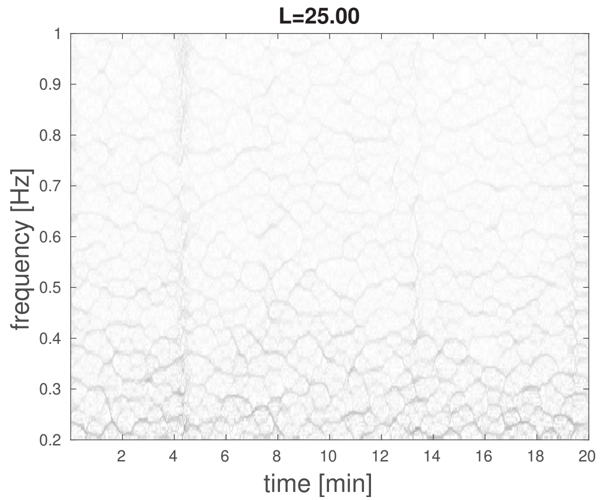

(t) second-order vertical synchrosqueezing

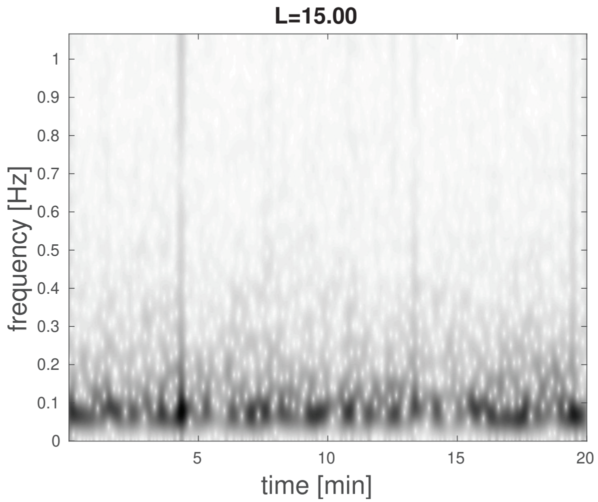

(u) spectrogram

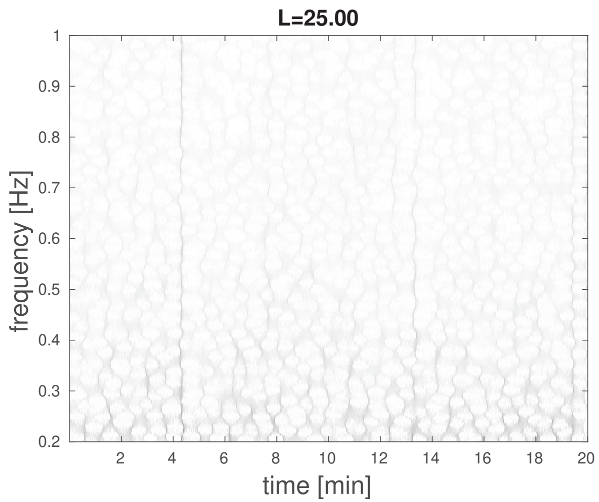

(v) time-reassigned synchrosqueezing

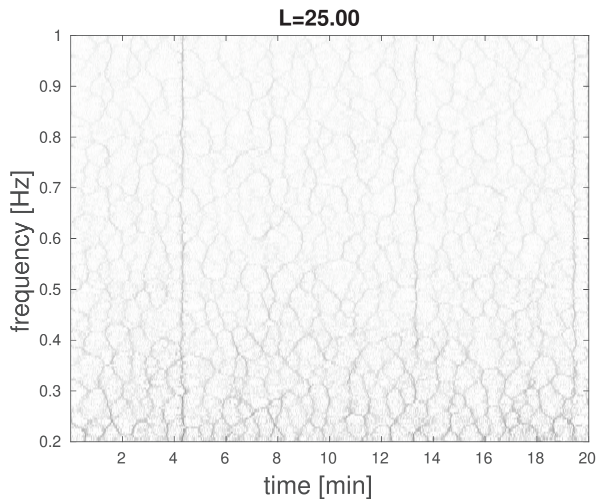

(w) second-order horizontal synchrosqueezing

Impulses detection

Proposed Saliency function

Defined as the root mean square of the marginal over frequency band $\Omega = [0.4; 1]$ Hz of the signal energy contained in the considered time-frequency representation.

$$G(t) = \left(\int_\Omega |TFR_x^h(t,\omega)|^2 d\omega \right)^{\frac{1}{2}}. \quad (26)$$

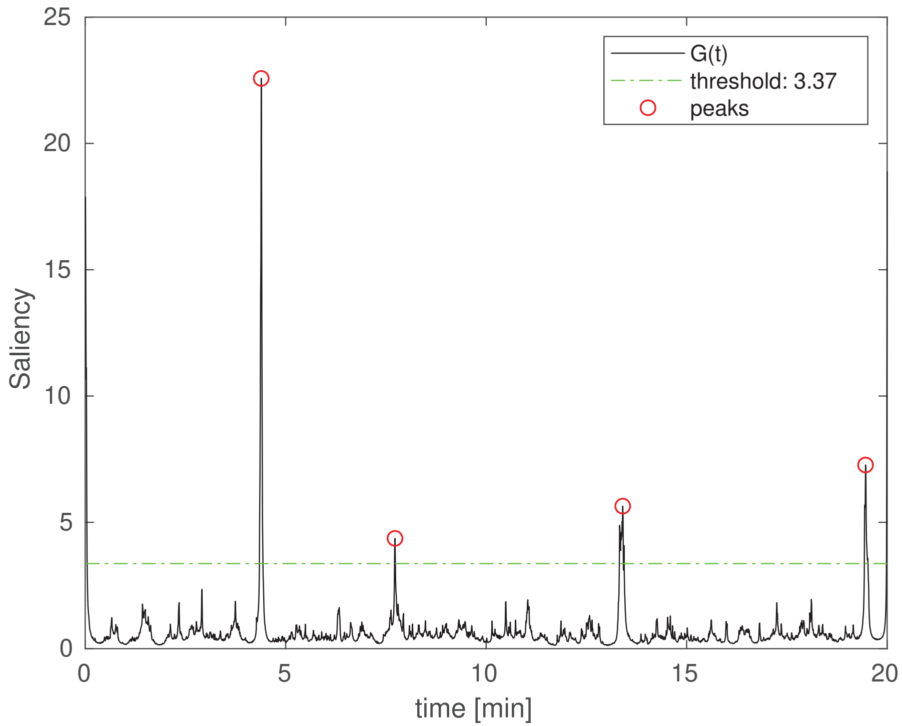

Figure : Result provided using the second-order horizontal synchrosqueezing.

Impulses disentangling

A binary masked version of the transform $S_x^h(t,\omega)$ can thus be computed using $G(t)$ as:

$$\hat{S}(t,\omega) = \begin{cases} S_x^h(t,\omega) & \text{if } G(t) > \Gamma \\ 0 & \text{otherwise} \end{cases} . \quad (27)$$

where Γ is a defined threshold.
Our numerical computation uses $\Gamma = 3.37$ which corresponds to 5 times the mean value of $G(t)$.

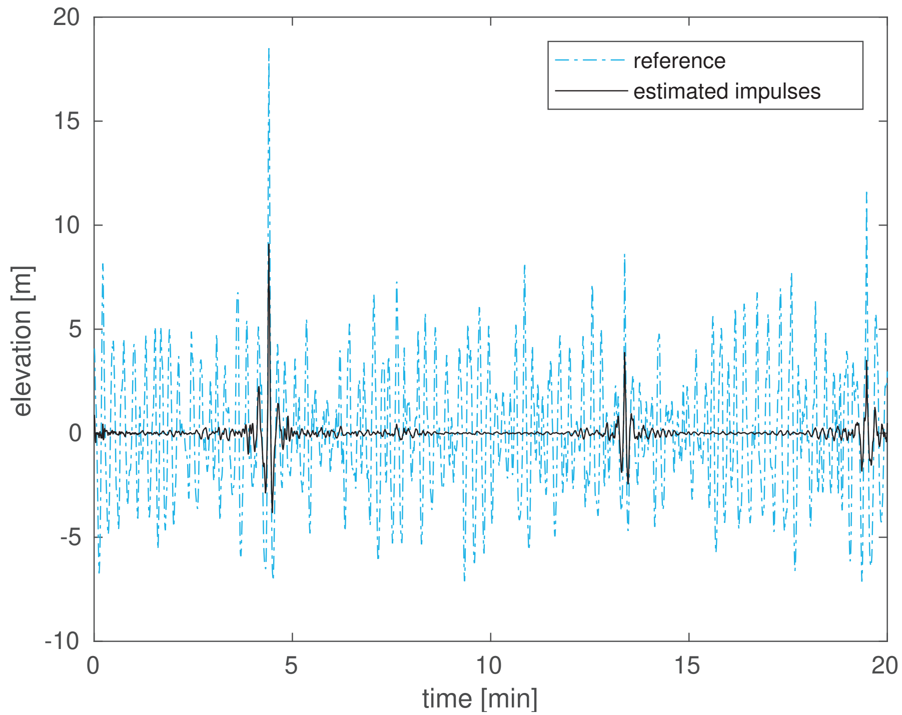

Figure : Draupner signal and recovered waveform of its impulsive components.

Contributions summary

- A novel horizontal synchrosqueezing method based on an enhanced group-delay estimator.
- Efficient computation from the STFT using specific analysis windows.
- New applicative results based on the Draupner wave signal.

Matlab code freely available on IEEE Code Ocean at: `http://fourer.fr/hsst`